Article

Not peer-reviewed version

MRI and Ultrasound of the Thoracolumbar Fascia in the Settings of Degenerative Spinal Diseases

Noa Martonovich , Clara De Luca , Caterina Fede * , Andrea Angelini , Pietro Ruggieri , Carla Stecco , Carmelo Pirri

Posted Date: 11 February 2026

doi: 10.20944/preprints202602.0846.v1

Keywords: low back pain; lumbar spinal stenosis; lumbar disc herniation; spondylolisthesis; ultrasonography; magnetic resonance imaging; thoracolumbar fascia; thickness

Article

MRI and Ultrasound of the Thoracolumbar Fascia in the Settings of Degenerative Spinal Diseases

Noa Martonovich [1,2], Clara De Luca [3,4], Caterina Fede [3]*, Andrea Angelini [4], Pietro Ruggieri [4], Carla Stecco [3] and Carmelo Pirri [3]

[1] Department of Orthopedic Surgery, Hillel Yaffe Medical Center, Hadera, Israel
[2] Rappaport Faculty of Medicine, Technion Israel Institute of Technology. Haifa, Israel
[3] Institute of Human Anatomy, Department of Neuroscience, University of Padova, Padova, Italy
[4] Orthopedics and Orthopedic Oncology, Department of Surgery, Oncology and Gastroenterology, University-Hospital of Padova, Padova, Italy
* Correspondence: caterina.fede@unipd.it; Phone: 00390498272308

Abstract

Background and Objectives: The thoracolumbar fascia (TLF) has been implicated in low back pain, but imaging-based characterization in specific degenerative lumbar pathologies—particularly in surgical cohorts—remains limited. To evaluate TLF thickness on Magnetic resonance imaging (MRI) and Ultrasound (US) across common lumbar pathologies, examine associations with age, body mass index, disability, and assess MRI–US agreement for TLF thickness. *Materials and Methods:* In this prospective single-centre cohort, adults scheduled for elective lumbar surgery underwent preoperative US (short- and long-axis at L3) and review of routine lumbar MRI (axial and sagittal T1-weighted measurements at L3) using standardized protocols. Disability was assessed using the Oswestry Disability Index (ODI). Group comparisons, correlation analyses, and intraclass correlation coefficients were used to evaluate between-diagnosis differences, patient-factor associations, and MRI–US agreement. *Results:* Thirty-seven patients were eligible (15 lumbar spinal stenosis, 5 discs herniations, 4 spondylolisthesis, 2 scoliosis, 9 revision surgeries, 2 trauma comparators). Median TLF thickness was 0.86 mm (0.16–1.40) on axial MRI, 1.12 mm (0.47–2.33) on sagittal MRI, 2.38 mm (1.01–5.91) on US short-axis, and 2.87 mm (1.12–5.74) on US long-axis. Axial MRI thickness differed across groups (p=0.010), driven by thinner measurements in trauma versus disc herniation (p=0.031); no significant group effects were observed on sagittal MRI or US. Age correlated positively with axial MRI thickness (p=0.021). No significant correlations were detected between ODI and TLF thickness on MRI or US. MRI–US agreement was poor, indicating the modalities are not interchangeable for TLF thickness measurement. *Conclusions:* TLF thickness measured on MRI and US did not consistently differentiate diagnostic groups and was not associated with disability. Thickness estimates differed substantially by modality, with poor MRI–US agreement. Larger studies with standardized acquisition and reliability testing are needed to clarify the clinical and mechanistic relevance of TLF imaging in degenerative lumbar disease and to determine whether it can support phenotype-based stratification within degenerative spine disease.

Keywords: low back pain; lumbar spinal stenosis; lumbar disc herniation; spondylolisthesis; ultrasonography; magnetic resonance imaging; thoracolumbar fascia; thickness

1. Introduction

Low back pain (LBP) is a major global burden. The number of people living with LBP increased by ~60% from 1990 to 2020, reaching an estimated 619 million people in 2020 and projected to rise to 843 million by 2050 [1,2]. While most cases are non-specific LBP (NSLBP), defined as pain not

 doi:10.20944/preprints202602.0846.v1

attributable to a specific pathoanatomical diagnosis, approximately 10–15% of casas are of identifiable spinal disorder, including, among others, stenosis, discopathies, sagittal and coronal imbalances disorders [3,4].

Degenerative spinal disorders are traditionally framed through osseous and disc-related changes (e.g., facet arthropathy, intervertebral discopathies, degenerative coronal and sagittal imbalances [5–7]), yet symptoms and disability do not always map neatly onto structural findings [8–10]. This gap has increased interest in complementary pain generators and biomechanical contributors beyond the vertebra–disc complex.

The thoracolumbar fascia (TLF) is a multilayered aponeurotic complex investing the paraspinal musculature and mechanically linking the spine to the abdominal wall and pelvis [11,12]. Structurally, the TLF is formed by an anterior and a posterior layer: the anterior layer inserts medially onto the lumbar transverse processes, whereas the posterior layer attaches to the lumbar supraspinous ligament, envelopes the erector spinae as a paraspinal retinacular sheath, and fuses laterally into a thickened lateral raphe that blends with the abdominal aponeuroses [12,13]. At the microscopic level, these layers can be resolved into multiple collagenous sublayers with differing fiber orientations, separated by thin loose connective tissue that permit interlaminar gliding [11].

Biomechanically, the posterior layer (with superficial and deep laminae) participates in load transfer across the lumbopelvic region; experimental loading demonstrates that tension applied via myofascial connections can deform the posterior TLF in a manner consistent with force transmission between the spine and lower limbs [14].

Immunohistochemical studies has demonstrated sensory innervation within the TLF, showing a dense network of free nerve endings, including nociceptive fiber populations with layer-specific distribution, supporting biological plausibility for the TLF as a pain-generating structure [15–20]. Experimental work further supports that nociceptive input from fascia can engage spinal nociceptive processing [21].

In vivo imaging studies in humans complement these findings: ultrasound (US) elasticity imaging has shown reduced shear strain of the TLF in chronic NSLB, and increased TLF thickness compared with healthy controls [22–24] Although methods and reporting remain heterogeneous [25].

However, most prior work has focused on NSLBP, and analogous evaluations in individuals with specific degenerative spinal pathologies are limited. The aim of this study was to characterize the TLF on ultrasound and MRI in participants with degenerative spinal disease.

2. Material and Methods

According to institutional policy and Helsinki Declaration rules, Ethical approval was not sought for the present study becuase it was an observational prospective study was conducted without treatment and only involved volunteers, Prior to all study procedures, written informed consent was obtained from all the volunteers after receiving detailed information regarding the study's objectives and MRI/US examination.

Consecutive patients were recruited from the Orthopedic Department of the University of Padova. Adults scheduled for elective lumbar surgery (decompression and/or fusion) were recruited and screened at preoperative admission the day before surgery.

Inclusion criteria: Age 18–80 years; male or female; chronic lumbar spinal pathology with clinical and radiological correlation, including Lumbar spinal stenosis (LSS), lumbar disc herniation (LDH), scoliosis, and degenerative spondylolisthesis. Patients undergoing revision surgery for these diagnoses were also eligible, limited to the first revision (i.e., second lumbar operation), performed for recurrent or persistent symptoms following the index procedure.

Exclusion criteria: known connective-tissue disorders or rheumatologic diseases affecting connective-tissue properties; active malignancy.

2.1. Clinical Assessment and Outcomes

 doi:10.20944/preprints202602.0846.v1

At admission (pre-operative), participants completed the Oswestry Disability Index (ODI), a validated 10-item instrument that quantifies low-back-pain–related disability on a 0–100% scale (higher scores = greater limitation) [26].

2.2. Ultrasound Protocol

On the pre-operative day, upon admission, participants underwent US assessment of the TLF. US was performed using a high-resolution system (Edge II, SonoSite, FUJIFILM, Bothell, WA, USA) with a 6–15 MHz linear transducer; the speed of sound was set to 1540 m/s (standard diagnostic setting) and B-mode depth to 30 mm. With the participant prone and relaxed, the L3 level was localized by palpating the posterior superior iliac crest to identify L5 and then counting cranially by palpation of the spinous processes to L3. Images were acquired bilaterally at L3 with the transducer placed parallel to the spine, approximately 2–3 cm lateral to the L3 spinous process. For each side, one short-axis and one long-axis image were obtained. The entire acquisition protocol was then repeated by a second operator, yielding 8 images per participant (2 sides × 2 planes × 2 operators). From this image pool, a stratified random subset was selected for analysis (one short-axis and one long-axis image per side) and exported to ImageJ (free available at https://imagej.net/ij/, accessed on 5th June 2025). TLF thickness was measured in ImageJ. To minimize local variability, each image was divided into three equal regions along the mediolateral axis. Within each region, three standardized measurement points (left, middle, right within that region) were used; thickness was measured perpendicular to the fascial plane at each point, and the three values were averaged to obtain a regional mean. The three regional means were then averaged to yield a single thickness value per image for analysis (Figure 1).

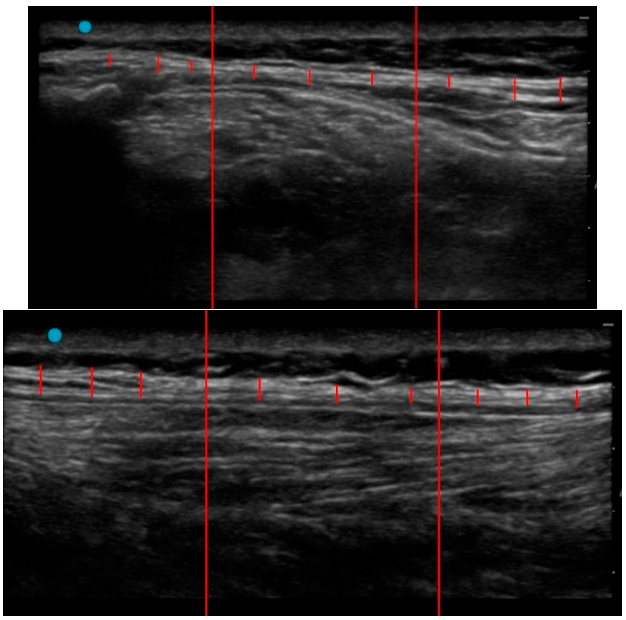

Figure 1. US assessment of TLF thickness at the L3 level. Representative short-axis (left) and long-axis (right) images obtained over the lumbar paraspinal region. Each image was divided into three equal mediolateral regions (vertical red lines). Within each region, TLF thickness was measured at three standardized points (red markers; 9 measurements per image) and averaged.

2.3. MRI Protocol

As part of the routine work-up, lumbar MRI (1.5 T) was obtained. T1-weighted sequences were analyzed using RadiAnt DICOM Viewer (64-bit), applying a standardized measurement protocol.

Axial plane: Measurements were performed at three L3 levels (superior endplate, mid-vertebral body, and inferior endplate). At each level, bilaterally, the region of interest was defined between (1) a line drawn parallel to the spinous process and (2) a line drawn at the longissimus–iliocostalis

 doi:10.20944/preprints202602.0846.v1

interface. This region was divided into three equal mediolateral thirds; within each third, thickness was measured at three predefined locations positioned at the inner thirds of that segment (left, middle, right), and averaged. The three regional means were then averaged to yield the value for analysis (Figure 2).

Sagittal plane: Two sagittal images immediately medial to the longissimus–iliocostalis border were selected. Two reference lines were drawn parallel to the superior and inferior endplates of L3, and the intervening region was divided into three equal thirds. Within each third, thickness was measured at three predefined locations (inner thirds: left, middle, right), averaged within each third, and then averaged across the three thirds to yield the value for analysis (Figure. 3).

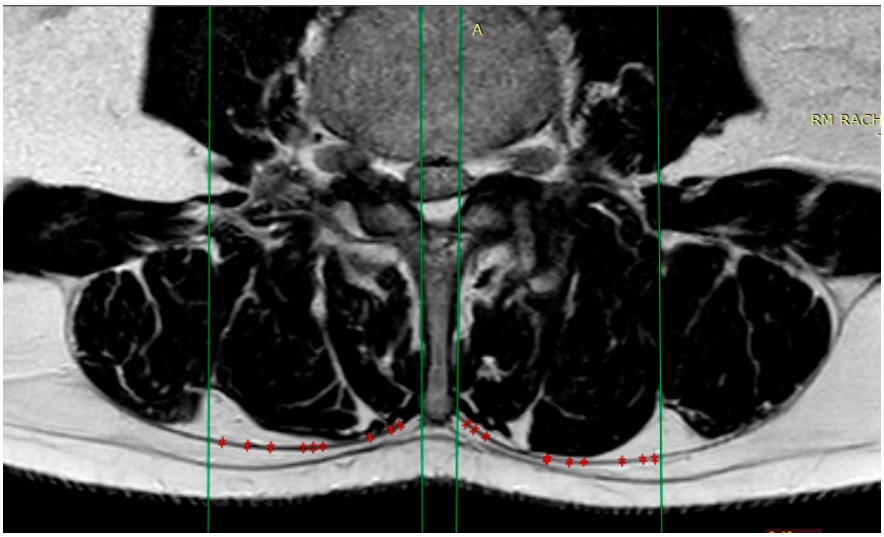

Figure 2. MRI assessment of TLF thickness in the axial plane at the L3 level. The green reference lines define the region of interest: one lines drawn parallel to the spinous process (medial boundaries) and a second line at each side drawn at the longissimus–iliocostalis interface (lateral boundaries). The red markers indicate individual caliper measurements of TLF thickness with three measurements per third.

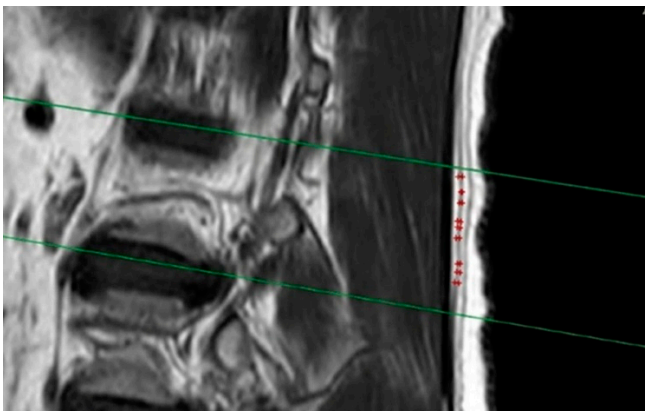

Figure 3. MRI assessment of TLF thickness in the sagittal plane at the L3 level. The upper and lower green lines mark the cranio-caudal boundaries of the L3 segment (above the superior endplate and below the inferior endplate). The red markers/short red lines indicate individual caliper measurements.

2.4. Statistical Analysis

Data were entered in Microsoft Excel and analyzed in JASP (v0.19.3). Continuous variables are summarized as mean ± SD (approximately normal) or median (range) (non-normal), and categorical variables as n (%). Normality was evaluated using the Shapiro–Wilk test and Q–Q plots; variance homogeneity was assessed with Levene's test. Group comparisons used Student's t test or one-way

 doi:10.20944/preprints202602.0846.v1

ANOVA for approximately normal data (Welch correction when variances were unequal) and Mann–Whitney U or Kruskal–Wallis tests for non-normal data, with appropriate post-hoc tests and multiplicity adjustment. Associations were examined using Pearson's r or Spearman's ϱ as appropriate. Two-tailed p values <0.05 were considered statistically significant. Agreement between MRI- and US-derived TLF thickness was evaluated with Bland–Altman analysis, reporting the average difference (MRI − US) and the 95% limits of agreement.

3. Results

3.1. Study Cohort

Thirty-seven patients were eligible. The cohort comprised 15 with LSS, 5 with LDH, 4 with spondylolisthesis, 2 with scoliosis, 9 revision surgeries with varied prior pathologies, and 2 trauma cases without a history of back pathology (comparative controls). The mean age was 54.68 ±14.29 years (range 18-77). Mean age differed by pathology (p<0.001). Ages were highest in revision (63.4±7.2 years) and stenosis (60.3±10.0) and lowest in trauma (21.0±1.4) and scoliosis (24.0±8.5). Post-hoc tests showed that the trauma and scoliosis groups were younger than the revision and stenosis groups, and the hernia group was older than scoliosis and trauma (all adjusted p<0.05). The gender distribution was 54% male / 46% female, and the mean BMI was 26.83 ± 7.04 kg/m² (16.41-39.04). Patients with degenerative diagnoses (LSS, scoliosis, LDH, spondylolisthesis) were further analysed as a single cohort (Group A) and showed a mean age of 54.23 ± 15 (range18-74), BMI of 26.75 ± 5.32 kg/m² (16.41-39.04), and gender distribution of 58% male and 42% female.

Overall demographics are summarized in Table 1.

Table 1. demographic data by pathology.

Group by pathology	N	Age		Gender	BMI		ODI	
		Mean ± SD	Range	Male (%)	Mean ± SD	Range	Mean ± SD	Range
Spinal stenosis	15	60.33± 10.03	29-70	53	26.26 ± 5.75	16.41-33.95	41.08 ± 10.44	24–62
Disc herniation	5	55.80± 16.73	42-74	80	26.31± 2.99	21.45-29.39	60.00 ± 16.38	46–78
Spondylolisthesis	4	44.50 ± 16.73	26-58	50	30.25 ± 6.34	24.16-39.04	34.00 ± 16.38	16–48
Scoliosis	2	24.00 ± 8.49	18-30	50	24.10 ± 5.52	20.00-28.00	n/a	n/a
Trauma	2	21.00 ± 1.41	20-22	50	24.83 ±5.23	19.04-32.41	n/a	n/a
Revision	9	63.44± 7.18	56-77	44	30.67± 4.32	22.84 - 37.33	53.72 ± 23.90	24–92
Total	37	54.68 ±14.29	18-77	54	26.83 ± 7.04	16.41-39.04	45.84 ± 17.38	16–92

Values are years for age, BMI in kg/m2, ODI in percentage. Gender values represent the percentage of male participants in each group (female = 100 − male). N = number of subjects. BMI= body mass index. ODI= Oswestry Disability Index. n/a= not applicable.

3.2. MRI-Derived TLF Thickness

25 lumbar MRIs were reviewed: LSS (n=11), LDH (n=5), spondylolisthesis (n=2), scoliosis (n=1), trauma (n=2), and revision (n=4). Overall median TLF thickness was 0.86 mm (range 0.16–1.40) on the axial plane and 1.12 mm (0.47–2.33) on the sagittal plane. Group A showed a median TLF thickness of 0.89 mm (range 0.16–1.40) on axial images and 1.16 mm (range 0.47–2.33) on sagittal images. Pathology-specific summaries are provided in Table 2.

On axial MRI, TLF thickness differed across diagnostic groups (p=0.010), although only disc herniation vs revision remained significant after post-hoc correction, with higher thickness in the revision group (p=0.031). On sagittal MRI, thickness did not differ across diagnostic groups (p=0.744).

Age was positively associated with TLF thickness on axial MRI (p = 0.021). A weaker, non-significant trend was observed on sagittal MRI (p = 0.503) (Figure 4). BMI did not correlate with MRI-

 doi:10.20944/preprints202602.0846.v1

derived thickness (axial: p = 0.863; sagittal: p = 0.946). (Figure 5). TLF thickness did not differ by gender on either axial plane (p = 0.141) or sagittal plane (p = 0.277).

Table 2. TLF thickness on MRI by pathology.

	TLF thickness on Axial Plane				TLF thickness on Sagittal Plane			
Diagnosis	N	Median	Range	P-value	N	Median	Range	P-value
Spinal Stenosis	11	0.99	0.75-1.35		11	1.36	0.47-2.33	
Spondylolisthesis	2	1.11	0.83-1.40		2	0.96	0.94-0.98	
Lumbar Disc Herniation	5	0.69	0.16-0.79	0.01	5	1.06	0.63-1.44	0.744
Trauma	2	0.70	0.64-0.76		2	1.14	0.81-1.48	
Revision	4	1.18	1.02-1.33		3	1.39	1.12-1.48	
Scoliosis	1	0.81	n/a	n/a	0	n/a	n/a	n/a
Total	**25**	**0.86**	**0.16-1.40**		**23**	**1.12**	**0.47-2.33**	

Values are median (range), in millimetres. N = number of subjects. n/a= not applicable. Thickness was measured on axial and sagittal planes. Group differences were examined with the Kruskal–Wallis test; two-tailed $p < 0.05$ was considered statistically significant.

3.3. Ultrasound-Derived TLF Thickness

27 patients underwent US: LSS (n=13), spondylolisthesis (n=3), LDH (n=2), scoliosis (n=1), revision (n=7) and trauma (n=1). Overall median TLF thickness was 2.38 mm (1.01-5.91) on the short axis and 2.87 mm (1.12-5.74) on the long axis. Pathology-specific summaries are provided in Table 3.

Among Group A, the median TLF thickness was 2.24 mm (range 1.01–5.91) in the short axis and 2.12 mm (range 1.12–4.49) in the long axis. Pathology-specific values are presented in Table 3. A weak, non-significant association between age and TLF thickness was observed—short axis (p = 0.434) and long axis (p = 0.355) (*Fig 4*). TLF thickness showed a trend toward higher values in females on both ultrasound planes, but this did not reach statistical significance (short axis: p = 0.067; long axis: p = 0.055).BMI showed a non-significant positive association with US short-axis TLF thickness (p = 0.223) and a very weak, non-significant association with US long-axis thickness (p = 0.486). Group differences were non-significant for the short axis (p = 0.231). Post-hoc tests suggested revision > spondylolisthesis (p = 0.041), but this did not survive Holm correction (p = 0.248). Long-axis US thickness did not differ significantly across diagnostic groups (p = 0.130). In post-hoc testing, revision showed higher ranks than spondylolisthesis (unadjusted p = 0.027), but this also did not remain significant after correction (p = 0.161).

Table 3. TLF thickness on US by pathology.

	TLF thickness on Short Axis (mm)				TLF thickness on Long Axis (mm)			
Diagnosis	N	Median	Range	P-value	N	Median	Range	P-value
Spinal Stenosis	13	2.48	1.01-5.91		9	2.12	1.12-4.49	
Spondylolisthesis	3	1.36	1.01-1.67	0.231	3	1.96	1.12-2.87	0.130
Lumbar Disc Herniation	2	2.25	2.13-2.38		2	2.61	1.66-3.56	
Revision	7	3.03	1.16-5.65		5	5.53	3.24-5.75	
Scoliosis	1	2.72	n/a	n/a	1	2.30	n/a	n/a
Trauma	1	1.33	n/a	n/a	1	3.72	n/a	n/a
Total	**26**	**2.38**	**1.01-5.91**		**27**	**3.56**	**1.12-8.56**	

Values are median (range), in millimetres. N = number of subjects per diagnosis. n/a= not applicable. Thickness was measured in short-axis and long-axis views. The p-values shown are from per-axis Kruskal–Wallis tests comparing diagnostic groups with adequate sample size (n ≥ 2); groups with n = 1 (lumbar disc herniation,

 doi:10.20944/preprints202602.0846.v1

trauma) were excluded from the inferential test and are marked n/a. Two-tailed $p < 0.05$ was considered statistically significant.

3.4. Inter-Method Comparison

Measurements derived from MRI and US showed substantial differences in mean values and ranges. Bland–Altman analysis showed that MRI produced lower TLF thickness values than US. For axial MRI versus short-axis US, the average difference was −1.191 mm, and for sagittal MRI versus long-axis US, the average difference was −1.789 mm.

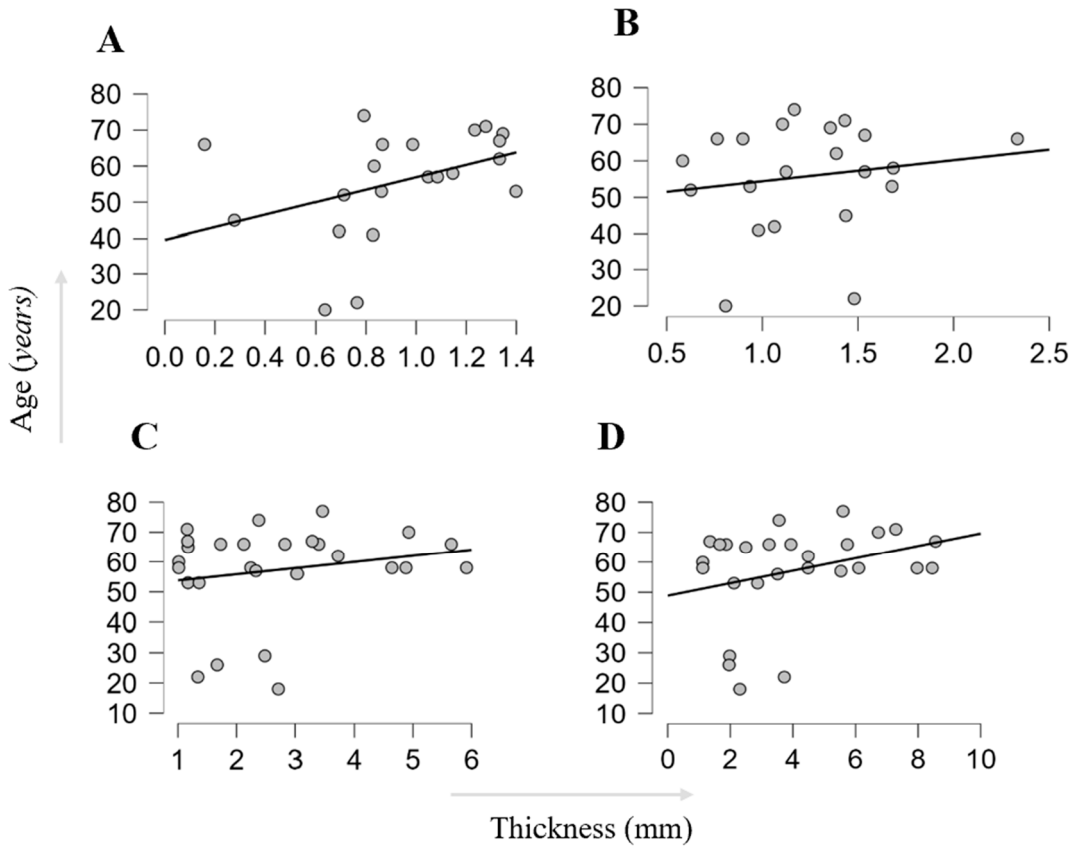

Figure 4. Scatterplots of age versus imaging-derived TLF thickness. (A) MRI axial, (B) MRI sagittal, (C) US short axis, and (D) US long axis. Each point represents one participant; solid lines show the fitted linear trend. X-axes denote TLF thickness (mm); y-axes denote age (years). Spearman correlations were: MRI axial $\rho = 0.500$, $p = 0.021$; MRI sagittal $\rho = 0.155$, $p = 0.503$; US short axis $\rho = 0.157$, $p = 0.434$; US long axis $\rho = 0.265$, $p = 0.182$. Only the axial MRI correlation reached statistical significance (two-tailed $\alpha = 0.05$).

 doi:10.20944/preprints202602.0846.v1

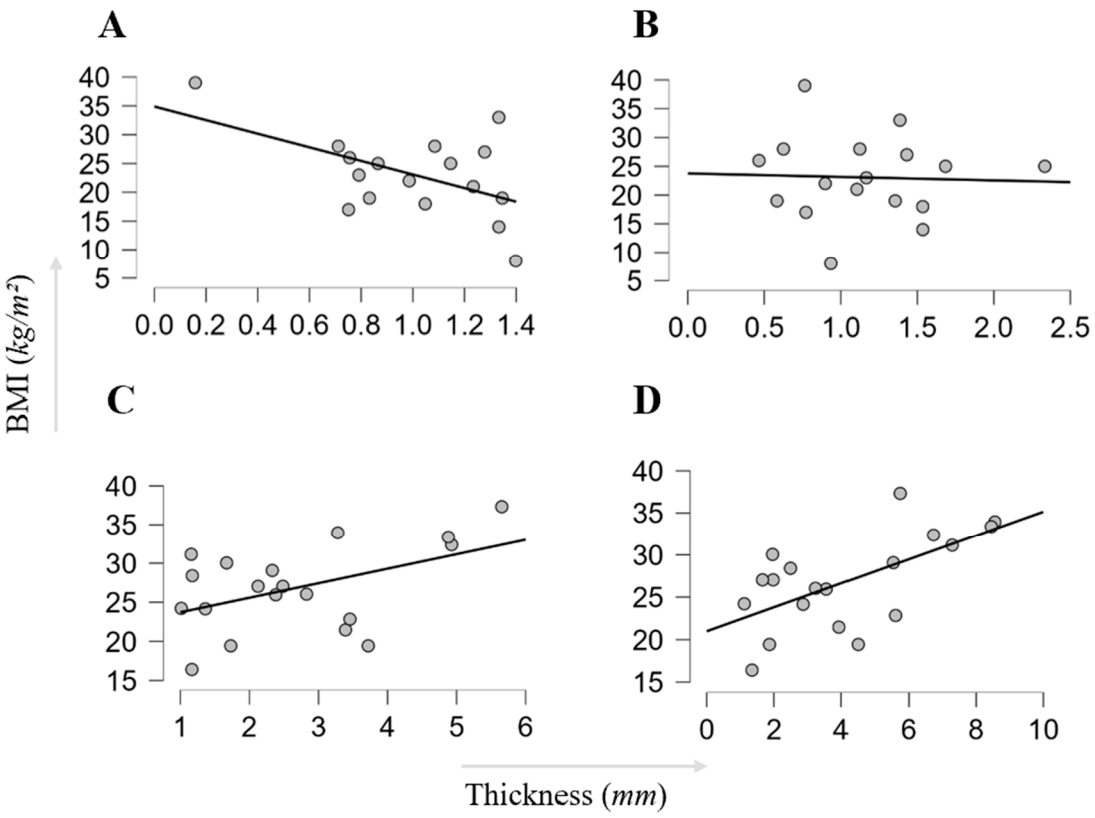

Figure 5. Scatterplots of BMI versus imaging-derived TLF thickness. (A) MRI axial, (B) MRI sagittal, (C) US short axis, and (D) US long axis. Each point represents one participant; solid lines show the fitted linear trend. X-axes denote TLF thickness (mm); y-axes denote BMI (kg/m²). Spearman correlations were: MRI axial ϱ = 0.039, p = 0.863; MRI sagittal ϱ = 0.016, p = 0.946; US short axis ϱ = 0.293, p = 0.223; US long axis ϱ = 0.586, p = 0.008. Only the long-axis US correlation reached statistical significance (two-tailed $\alpha = 0.05$).

3.5. Clinical Assessment

The ODI was available for 26 participants; pathology-specific values are shown in *Table 1*. Mean ODI did not differ significantly between diagnostic groups (p=0.115); Across imaging measures, no significant correlations with ODI were detected: axial MRI (p = 0.146; negative trend), sagittal MRI (p = 0.694), US short-axis (p = 0.394), and US long-axis (p = 0.558). *Figures 6* displays the corresponding scatterplots.

 doi:10.20944/preprints202602.0846.v1

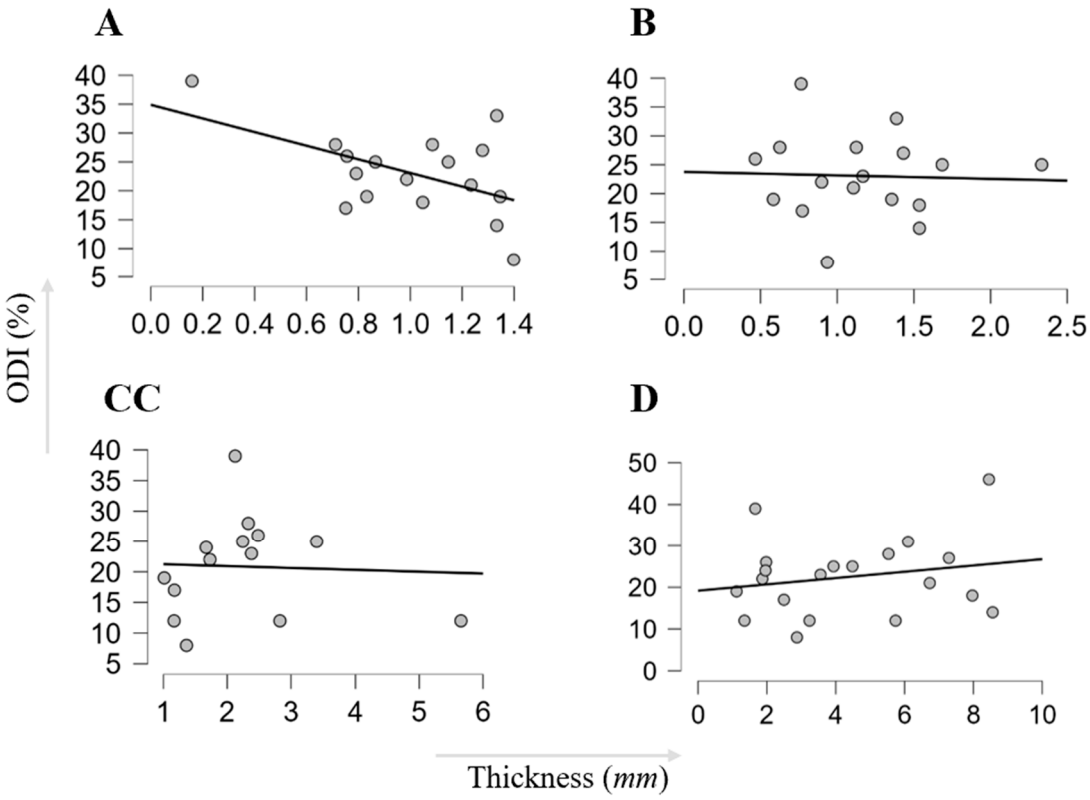

Figure 6. Scatterplots of ODI versus imaging-derived TLF thickness. (A) MRI axial, (B) MRI sagittal, (C) US short axis, and (D) US long axis. The x-axes show thickness measurements; the y-axes show ODI scores. Each dot represents one participant; the solid line indicates the fitted linear trend. No significant associations were observed (two-tailed Spearman): MRI axial $\varrho = -0.368$, $p = 0.146$; MRI sagittal $\varrho = -0.103$, $p = 0.694$; US short axis $\varrho = 0.140$, $p = 0.556$; US long axis $\varrho = 0.139$, $p = 0.558$.

4. Discussion

This study evaluated whether in vivo TLF thickness, measured using standardized protocols on MRI and US, differs across common lumbar pathologies and relates to patient factors and disability.

TLF thickness measured on MRI and US was not associated with disability (ODI) in this cohort. Prior US studies in chronic NSLBP have variably reported increased TLF thickness compared with asymptomatic controls [27]. This lack of association does not necessarily contradict prior literature: in NSLBP, where no single structural diagnosis dominates, a subset of patients may have pain and disability more closely linked to myofascial factors, and a "fascial subgroup" has been proposed [28,29]. By contrast, in patients with defined degenerative spine pathology, ODI is likely influenced primarily by competing drivers such as neural compression, mechanical instability, and pain chronicity-related factors. These dominant determinants can reduce the observable contribution of fascial morphology to functional limitations, making a correlation between TLF thickness and ODI less likely to emerge, particularly in small, heterogeneous surgical samples.

When contextualized against prior literature, in our degenerative surgical cohort (Group A, *Table 4*), mean TLF thickness was 2.53 ± 1.44 mm in the short axis and 2.49 ± 1.14 mm in the long axis. These values are higher than those reported by Pirri et al., both in their NSLBP group (means ~1.95–2.13 mm short axis and ~2.09–2.27 mm long axis) and in healthy controls (~1.6–1.7 mm short axis and ~1.75–1.96 mm long axis) [24]. Taken together, this cross-study comparison suggests that TLF thickness may be greater in degenerative spine disease cohorts than in NSLBP, a hypothesis that warrants direct testing.

On MRI, Caron et al. reported no differences in TLF morphology (e.g., layer lengths, circumference, and epimuscular fat contact) between individuals with chronic LBP and healthy

 doi:10.20944/preprints202602.0846.v1

controls, and no association with pain severity [30]. In contrast, Adamietz et al. reported substantially greater TLF thickness than in our cohort—approximately twice our median axial values [31]. This divergence is likely driven, at least in part, by methodological differences in imaging and measurement definitions, such as MRI sequence, anatomical level and plane sampled, and whether only the posterior TLF lamina was measured or also adjacent epimysium.

Wilke et al.[32] reported clear age- and BMI-related differences in US-derived thickness. In our surgical degenerative cohort, associations with age were weaker overall and reached statistical significance only for axial-plane MRI thickness, whereas US-derived thickness showed no significant correlation with age. BMI showed a clearer association with US-derived long-axis thickness than with short-axis. These differences are plausibly explained by population and study-design differences.

Across planes and modalities, group differences were inconsistent. Axial MRI showed a statistically significant group effect that was largely driven by thinner measurements in trauma compared with disc herniation; this contrast was not reproduced on sagittal MRI or on US, and no coherent ranking of thickness by diagnosis emerged. Directionally, revision cases tended to have higher thickness values, whereas trauma (on MRI) and spondylolisthesis (on US) tended to be lower, but these patterns were not stable across modalities and largely did not persist after correction for multiple comparisons. Given the small and uneven subgroup sizes, these comparisons should be interpreted cautiously. The absence of consistent between-group differences across modalities may reflect limited statistical power (type II error), while isolated significant findings may represent chance associations (type I error). Accordingly, our results do not provide strong evidence that TLF thickness differs systematically by diagnosis in this cohort, and larger studies are needed.

While both US and MRI have been successfully used to assess deep fasciae (including the TLF), with good reproducibility reported for US thickness measures and demonstrated feasibility of MRI-based visualization [25,33], in this cohort, MRI–US agreement for thickness was poor , indicating the two modalities are not interchangeable for this metric. US yielded greater TLF thickness than MRI in our cohort, which is expected given: (i) anisotropy—small probe-angle deviations (±5°) materially alter deep-fascia thickness [34]; (ii) probe compression, which can distort soft tissues and reduce apparent adipose layers by ~25–37% [35]; (iii) positioning—routine spine MRI is supine whereas our US was prone, changing tissue tension and gravitational load [36,37]; and (iv) US beam/slice-thickness artefacts, which can blur adjacent layers and inflate apparent thickness. Moreover, MRI frequently showed deep adipose fibrosis and infiltration between TLF and epimysium; on US, especially where layers adhere, these tissues may be conflated with the TLF band, contributing to thicker US readings [38] (see Figures 7-8).

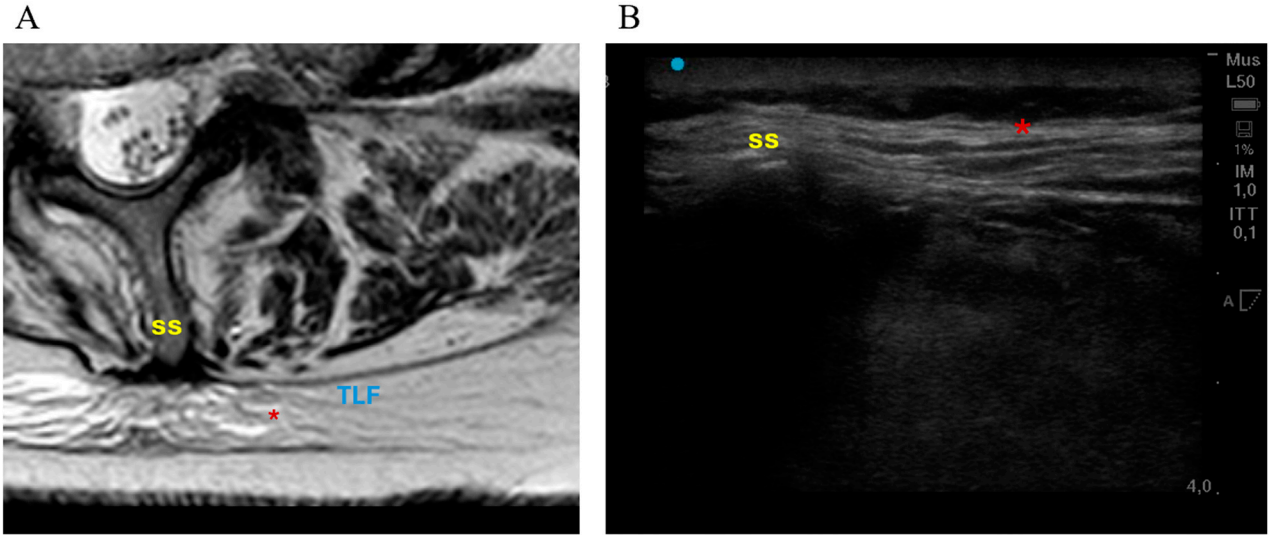

 doi:10.20944/preprints202602.0846.v1

Figure 7. MRI (A) and US (B) at the L3 level of a female subject. SS = spinous process. On MRI, fibrosis of the deep adipose tissue is visible (*), which may appear as part of the thoracolumbar fascia (TLF) on the corresponding US image, creating an artifact of increased thickness.

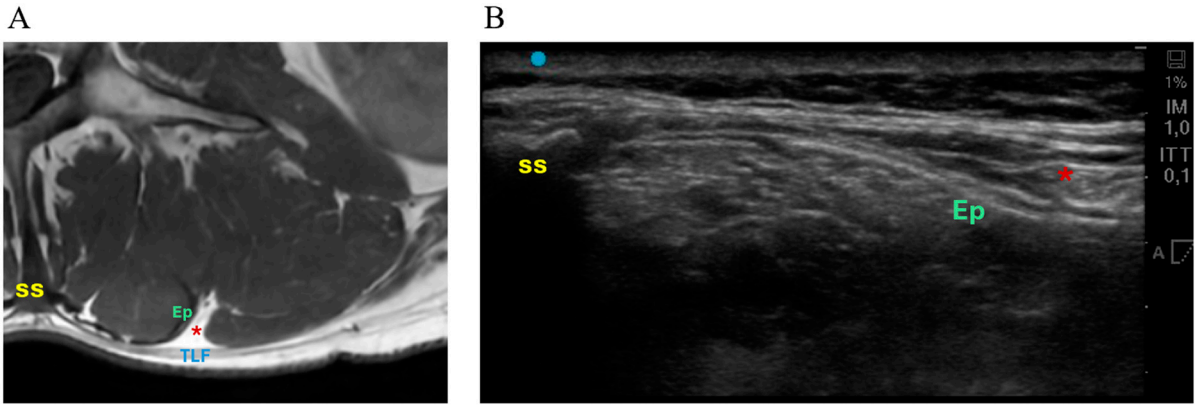

Figure 8. MRI (A) and US (B) at the L3 level of a male subject. SS = spinous process; Ep = epimysium of the erector spinae. On MRI, a triangle-shaped infiltration between the thoracolumbar fascia (TLF) and the epimysium (*) is visible, which may have been interpreted as part of the TLF on the US image.

Associations with patient factors also differed by modality. Age showed a modest positive association with TLF thickness on MRI, whereas no age effect was evident on US. MRI may capture more robustly age-related ECM remodeling, while US measurements are highly susceptible to plane and probe-pressure dependencies (anisotropy, compression)[33,34,39,40]. In contrast, BMI did not influence MRI-derived TLF thickness but showed a strong positive correlation on the US long axis and a weaker, non-significant trend on the short axis. This divergence likely reflects a combination of true biologic co-variation, such as greater adjacent adiposity and extracellular-matrix remodeling with higher BMI [41,42], and US-specific measurement dependencies at greater fat depths (attenuation, beam aberration from speed-of-sound mismatch, and angle/pressure effects [43–45]), which do not affect MRI to the same extent. Taken together, these findings reinforce that MRI- and US-based thickness estimates are not interchangeable and suggest that age and BMI should be included as covariates in future work.

Limitations include the single-centre surgical design and relatively small, imbalanced diagnostic subgroups, reducing power for between-diagnosis comparisons and increasing the risk of unstable estimates. Preoperative MRI and/or US were not available for all participants, for example, in trauma presentations, in patients who consented but could not tolerate the prone positioning required for ultrasonography, or when the MRI did not include the study level. In addition, the trauma and scoliosis subgroups were substantially younger than the remaining diagnostic groups in this cohort, introducing age as a major confounder for between-group differences in TLF thickness. MRI examinations were obtained as part of clinical care and may have varied in acquisition parameters, which can influence measurement precision. US measurements are operator- and technique-sensitive; in this study, imaging measurements were performed by a single unblinded rater and no formal inter-rater reliability assessment was performed, which may introduce measurement bias. Finally, the absence of a truly healthy control group limits inference about how thickness values compare to asymptomatic populations. Future studies should prioritize larger cohorts, standardized MRI sequences and US acquisition, and reliability testing, and should expand imaging beyond thickness alone (e.g., echogenicity/texture measures on US, elastography, MRI-based characterization of adjacent tissue planes and signal features). Longitudinal follow-up could clarify whether baseline fascial imaging features relate to postoperative trajectories of pain, function, or treatment response. Future studies should evaluate whether a TLF-involved phenotype exists within degenerative lumbar disease and whether stratifying patients by fascial involvement improves clinical interpretability beyond diagnostic categories

 doi:10.20944/preprints202602.0846.v1

Table 4. TLF Thickness of Group A across different modalities.

	Mean	Standart Deviation	Median (mm)	Range (mm)
MRI axial	0.89	0.33	0.89	0.16–1.40
MRI sagittal	1.16	0.48	1.16	0.47–2.33
US short axis	2.53	1.44	2.24	1.01–5.91
US long axis	2.49	1.14	2.12	1.12–4.49

5. Conclusions

In this surgical cohort with common lumbar pathologies, TLF thickness measured on MRI and US did not consistently distinguish diagnostic groups and showed no clear association with disability. Compared with previously published US data in NSLBP and asymptomatic cohorts, our degenerative surgical cohort demonstrated higher TLF thickness values, although cross-study comparisons are limited and warrant direct head-to-head confirmation. Thickness estimates differed substantially by modality, with poor MRI–ultrasound agreement, indicating that the two techniques are not interchangeable for TLF thickness measurement.

Author Contributions: Conceptualization, N.M. and C.S.; Methodology, C.P.; N.M. and C. D.L.; Software, N.M., C.D.L. and C.S.; Validation, C.P. and C.S.; Formal Analysis, N.M.; Investigation, C.P., N.M. and C.D.L.; Resources, C.P., A.A. and P.R.; Data Curation, N.M., C.F., C.D.L. and C.S.; Writing – Original Draft Preparation, N.M.; Writing – Review & Editing, C.F. and C.S.; Visualization, N.M.; Supervision, C.S., A.A. and P.R.

Funding: This research received no external funding.

Institutional Review Board Statement: The study was conducted in accordance with the Declaration of Helsinki. Ethical approval was not sought for the present study because it was an observational prospective study was conducted without treatment and only involved volunteers.

Informed Consent Statement: Informed consent was obtained from all subjects involved in the study.

Data Availability Statement: The data presented in this study are available on request from the corresponding author due to privacy and ethical reasons.

Conflicts of Interest: The authors declare no conflict of interest.

References

1. Hartvigsen, J.; Hancock, M.J.; Kongsted, A.; Louw, Q.; Ferreira, M.L.; Genevay, S.; Hoy, D.; Karppinen, J.; Pransky, G.; Sieper, J.; Smeets, R.J.; Underwood, M.; Lancet Low Back Pain Series Working Group. What low back pain is and why we need to pay attention. *Lancet* **2018**, *391*, 2356-2367.
2. Ferreira, M.L.; De Luca, K.; Haile, L.M.; Steinmetz, J.D.; Culbreth, G.T.; Cross, M.; et al. Global, regional, and national burden of low back pain, 1990–2020, its attributable risk factors, and projections to 2050: a systematic analysis of the Global Burden of Disease Study 2021. *Lancet Rheumatol* **2023**, *5*, e316-e329.
3. Traeger, A.; Buchbinder, R.; Harris, I.; Maher, C. Diagnosis and management of low-back pain in primary care. *CMAJ* **2017**, *189*, E1386-E1395. d
4. Deyo, R.A.; Weinstein, J.N. Low Back Pain. *N Engl J Med* **2001**, *344*, 363-370.
5. Andaloro, A. Lumbar spinal stenosis. *JAAPA* **2019**, *32*, 49-50.
6. Akuthota, V.; Lento, P.; Sowa, G. Pathogenesis of lumbar spinal stenosis pain: why does an asymptomatic stenotic patient flare? *Phys Med Rehabil Clin N Am* **2003**, *14*, 17-28.
7. Ansari, K.; Singh, M.; McDermott, J.R.; Gregorczyk, J.A.; Balmaceno-Criss, M.; Daher, M.; McDonald, C.L.; Diebo, B.G.; Daniels, A.H. Adolescent idiopathic scoliosis in adulthood. *EFORT Open Rev* **2024**, *9*, 676-684.
8. Brinjikji, W.; Luetmer, P.H.; Comstock, B.; Bresnahan, B.W.; Chen, L.E.; Deyo, R.A.; Halabi, S.; Turner, J.A.; Avins, A.L.; James, K.; Wald, J.T.; Kallmes, D.F.; Jarvik, J.G. Systematic literature review of imaging features of spinal degeneration in asymptomatic populations. *AJNR Am J Neuroradiol* **2015**, *36*, 811-6.
9. Benzakour, T.; Igoumenou, V.; Mavrogenis, A.F.; Benzakour, A. Current concepts for lumbar disc herniation. *Int Orthop* **2019**, *43*, 841-851.

 doi:10.20944/preprints202602.0846.v1

10. Sekiguchi, M. The Essence of Clinical Practice Guidelines for Lumbar Spinal Stenosis, 2021: 1. Definition, Epidemiology, and Natural History. *Spine Surg Relat Res* **2023**, *7*, 298-299.
11. Benetazzo, L.; Bizzego, A.; De Caro, R.; Frigo, G.; Guidolin, D.; Stecco, C. 3D reconstruction of the crural and thoracolumbar fasciae. *Surg Radiol Anat* **2011**, *33*, 855-862.
12. Willard, F.H., Vleeming, A., Schuenke, M.D., Danneels, L., Schleip, R. The thoracolumbar fascia: anatomy, function and clinical considerations. *J Anat* **2012**, *221*, 507-536.
13. Schuenke, M.D.; Vleeming, A.; Van Hoof, T.; Willard, F.H. A description of the lumbar interfascial triangle and its relation with the lateral raphe: anatomical constituents of load transfer through the lateral margin of the thoracolumbar fascia. *J Anat* **2012**, *221*, 568-576.
14. Vleeming, A.; Pool-Goudzwaard, A.L.; Stoeckart, R.; Van Wingerden, J.P.; Snijders, C.J. The Posterior Layer of the Thoracolumbar Fascia | Its Function in Load Transfer From Spine to Legs. *Spine* **1995**, *20*, 753-758.
15. Tesarz, J.; Hoheisel, U.; Wiedenhöfer, B.; Mense, S. Sensory innervation of the thoracolumbar fascia in rats and humans. *Neuroscience* **2011**, *194*, 302-308.
16. Corey, S.M.; Vizzard, M.A.; Badger, G.J., Langevin, H.M. Sensory innervation of the nonspecialized connective tissues in the low back of the rat. *Cells Tissues Organs* **2011**, *194*, 521-530.
17. Fede, C.; Petrelli, L.; Guidolin, D.; Porzionato, A.; Pirri, C.; Fan, C.; De Caro, R.; Stecco, C. Evidence of a new hidden neural network into deep fasciae. *Sci Rep* **2021**, *11*, 12623.
18. Yahia, L.; Rhalmi, S.; Newman, N.; Isler, M. Sensory innervation of human thoracolumbar fascia: An immunohistochemical study. *Acta Orthop Scand* **1992**, *63*, 195-197.
19. Mense, S.; Hoheisel, U. Evidence for the existence of nociceptors in rat thoracolumbar fascia. *J Bodyw Mov Ther* **2016**, *20*, 623-628.
20. Mense, S. Innervation of the thoracolumbar fascia. *Eur J Transl Myol* **2019**, *29*.
21. Hoheisel, U.; Mense, S. Inflammation of the thoracolumbar fascia excites and sensitizes rat dorsal horn neurons. *Europ J Pain* **2015**, *19*, 419-428.
22. Langevin, H.M.; Stevens-Tuttle, D.; Fox, J.R.; Badger, N.A.; Bouffard, N.A.; Krag, M.H.; Wu, J.; Henry, S.M. Ultrasound evidence of altered lumbar connective tissue structure in human subjects with chronic low back pain. *BMC Musculoskelet Disord* **2009**, *10*, 151.
23. Langevin, H.M.; Fox, J.R.; Koptiuch, C.; Badger, G.J.; Greenan-Naumann, A.C.; Bouffard, N.A.; Konofagou, E.E.; Lee, W.N.; Triano, J.J.; Henry, S.M. Reduced thoracolumbar fascia shear strain in human chronic low back pain. *BMC Musculoskelet Disord* **2011**, *12*, 203.
24. Pirri, C.; Pirri, N.; Guidolin, D.; Macchi, V.; Porzioanto, A.; De Caro, R.; Stecco, C. Ultrasound Imaging of Thoracolumbar Fascia Thickness: Chronic Non-Specific Lower Back Pain versus Healthy Subjects; A Sign of a "Frozen Back"? *Diagnostics* **2023**, *13*, 1436.
25. Pirri, C.; Pirri, N.; Macchi, V.; Porzionato, A.; De Caro, R.; Stecco, C. Ultrasound Imaging of Thoracolumbar Fascia: A Systematic Review. *Medicina* **2024**, *60*, 1090.
26. Fairbank, J.C.; Couper, J.; Davies, J.B.; O'Brien, J.P. The Oswestry low back pain disability questionnaire. *Physiother* **1980**, *66*, 271-273.
27. Bonaldi, L.; Berardo, A.; Stecco, A.; Stecco, C.; Fontanella, C.G. Assessment of the Fascial System Thickness in Patients with and Without Low Back Pain: A Narrative Review. *Diagnostics* **2025**, *15*, 2059.
28. Saragiotto, B.T.; Maher, C.G.; Hancock, M.J.; Koes, B.W. Subgrouping Patients With Nonspecific Low Back Pain: Hope or Hype? *J Orthop & Sports Physical Ther* **2017**, *47*, 44-48.
29. Wilke, J.; Schleip, R.; Klingler, W.; Stecco, C. The Lumbodorsal Fascia as a Potential Source of Low Back Pain: A Narrative Review. *Biomed Res Int* **2017**, *2017*, 5349620.
30. Caron, F.P.; Martin Smith, C.; Naghdi, N.; Iorio, O.C.; Bertrand, C.; Fortin, M. Morphological characteristics of the thoracolumbar fascia: relationship to chronic low back pain and back extension strength. *Eur Spine J* **2025**, *34*, 2562-2570.
31. Adamietz, B.; Schönberg, S.O.; Reiser, M.; Uder, M.; Frank, A.; Strecker, R.; Weiß, C.; Heiss, R. Visualization of the epimysium and fascia thoracolumbalis at the lumbar spine using MRI. *Radiologe* **2021**, *61*, 49-53.
32. Wilke, J.; Macchi, V.; De Caro, R.; Stecco C. Fascia thickness, aging and flexibility: is there an association? *J Anat* **2019**, *234*, 43-49.

 doi:10.20944/preprints202602.0846.v1

33. Serhal, A.; Adams, B.; Omar, I.; Deshmukh, S. Fascia lata attachment at the iliac crest: refining our diagnostic criteria of injury on magnetic resonance imaging. *Br J Radiol* **2020**, *93*, 20200187.
34. Pirri, C.; Pirri, N.; Guidolin, D.; De Rose, E.; Macchi, V.; Porzionato, A.; De Caro, R.; Stecco, C. The (ProteUS) Anisotropy Effect in Deep Fascia Ultrasonography: The Impact of Probe Angulation on Echogenicity and Thickness Assessments. *Life (Basel)*. **2025**, *15*, 822.
35. Ponti, F.; De Cinque, A.; Fazio, N.; Napoli, A.; Guglielmi, G.; Bazzocchi, A. Ultrasound imaging, a stethoscope for body composition assessment. *Quant Imaging Med Surg* **2020**, *10*, 1699-1722.
36. Calle-Toro, J.S.; Maya, C.L.; Gorfu, Y.; Dunn, E.; Darge, K.; Back, S.J. Supine versus prone positioning for ultrasound evaluation of postnatal urinary tract dilation in children. *Pediatr Radiol* **2020**, *50*, 357-362.
37. Cronin, C.G.; Lohan, D.G.; Mhuircheartaigh, J.N.; McKenna, D.; Alhajeri, N.; Roche, C.; Murphy, J.M. MRI Small-Bowel Follow-Through: Prone Versus Supine Patient Positioning for Best Small-Bowel Distention and Lesion Detection. *AJR Am J Roentgenol* **2008**, *191*, 502-6.
38. Baad, M.; Lu, Z.F.; Reiser, I.; Paushter, D. Clinical Significance of US Artifacts. *RadioGraphics* **2017**, *37*, 1408-1423.
39. Zullo, A.; Fleckenstein, J.; Schleip, R.; Hoppe, K.; Wearing, S.; Klingler, W. Structural and Functional Changes in the Coupling of Fascial Tissue, Skeletal Muscle, and Nerves During Aging. *Front Physiol* **2020**, *11*, 592.
40. Cebula, A.; Cebula, M.; Czajkowska, M.; Gruszczyńska, K.; Kopyta, I. Influence of the physical pressure of an ultrasound probe on shear-wave elastography measurements of the gastrocnemius muscle in a paediatric population: a non-interventional cohort study. *Pol J Radiol* **2024**, *89*, e24-e29.
41. Sun, K.; Li, X.; Scherer, P.E. Extracellular Matrix (ECM) and Fibrosis in Adipose Tissue: Overview and Perspectives. *Compr Physiol* **2023**, *13*, 4387-4407.
42. Jha, D.K.; Wongkaewpotong, J.; Chuckpaiwong, B. Effect of Age and BMI on Sonographic Findings of Plantar Fascia. *J Foot Ankle Surg* **2023**, *62*, 125-128.
43. Neto Müller, J.; Lanferdini, F.J.; Passos Karam, J.Y.; de Brito Fontana, H. Examination of the confounding effect of subcutaneous fat on muscle echo intensity utilizing exogenous fat. *Appl Physiol Nutr Metab* **2021**, *46*, 473-478.
44. Uppot, R.N. Technical challenges of imaging & image-guided interventions in obese patients. *Br J Radiol* **2018**, *91*, 20170931.
45. Canever, J.B.; Lanferdini, F.J.; de Moura, B.M.; Diefenthaeler, F.; Lima, K.M.M.E. Influence of subcutaneous adipose thickness and dominance on reliability of quadriceps muscle quality in healthy young individuals. *J Ultrasound* **2021**, *25*, 513-519.